CSCE Annual Conference

Growing with youth – Croître avec les jeunes

Laval (Greater Montreal)

June 12 - 15, 2019

PERFORMANCE OF THREE DOWEL TYPE STEEL CONNECTORS ON THE STRENGTH AND STIFFNESS OF HYBRID STEEL DECK TO WOOD FRAME DIAPHRAGMS

Boucher, S.[1] and Lamarche, C.P.[1,2]
[1] Université de Sherbrooke, Canada
[2] Charles-Philippe.Lamarche@USherbrooke.ca

Abstract: An increasing number of hybrid constructions are being designed and built and there is a need to better understand their structural behavior. This paper presents part of a research project about the structural behavior of roof or floor diaphragms made of lightweight steel decks that are attached to a wood structure. The main objective of this paper is to study the strength and stiffness of shear connections using three different dowel type connectors that would potentially allow the construction of structurally and economically efficient steel/wood diaphragms. Steel to wood shear tests were performed on the connections to characterize the failure mode, strength and slip modulus for each connection. Attempts to predict the lateral yield strength and slip modulus of the tested connections using equations proposed in the literature are also presented. Based on the experimental results, the strength and stiffness of steel deck to wood frame diaphragms are presented in order to evaluate whether the connections investigated yield to efficient diaphragm design that could be used in a practical context.

1 INTRODUCTION

An increasing number of hybrid constructions are being designed and built and there is a need to better understand their structural behavior. This paper presents part of a research project that explores the possibility of using different types of connectors to efficiently connect steel decks (corrugated metal sheets) on a wood structure to create roof or floor diaphragms. The strength and stiffness of a steel deck diaphragm depend on the thickness, type of deck and the mechanical properties of the connectors at the supports (metal sheet to structure) and at side joints (metal sheet to metal sheet). The state of the art on this specific combination of materials and structural components is limited. The design equations to evaluate the strength and stiffness of roof and floor diaphragms made from steel decks that are attached to a steel structure are well developed and readily available (Luttrell 2015, AISI S310-13 2013). The main difference between a steel deck to steel structure diaphragm and a steel deck to wood structure diaphragm is the metal sheet to structure connections. The specific influence of the type of connector used to join the two aforementioned components is a key factor in determining the in-plane structural behavior of the diaphragms. Little information is provided in current design standards to predict the strength and stiffness of steel deck to wood connections.

The main objective of this paper is to study the strength and stiffness of three different dowel type connectors that would potentially allow the construction of structurally and economically efficient steel deck to wood frame diaphragms. In order to achieve this objective, attempts to predict the lateral yield strength

and slip modulus of connections using equations proposed in the literature are presented. Lateral loading test results of steel to wood connections in single shear are presented. The failure modes, strength and slip modulus (shear stiffness) of each type of connector are compared to the prediction equations. Finally, based on the experimental test results, the potential strength and stiffness of steel deck to wood frame diaphragms are calculated in order to evaluate whether the proposed connections are efficient and usable in a practical context.

2 STRENGTH AND STIFFNESS PREDICTIONS OF STEEL DECK TO WOOD CONNECTIONS

In order to connect a steel deck to wood structural members, three different types of dowel type connector were considered: 1) common 1 ½ in. gauge #11 roofing nail (Nail #11); 2) 1 ½ in. Simpson Strong-Tie HJ (SST-HJ) roofing and sheet metal screw with built in washer (Simpson Strong-Tie 2018); and 3) 3 in. large head Rothoblaas TBS 6x80 (Rhoto-TBS) structural flange head screw with built in washer (Rothoblaas 2018). The dimensions and nominal yield stress of the connectors are presented in Table 1, where L is the length of the connector, L_t is the threaded length, d_i is the minor diameter, d_e is the major diameter, d_h is the diameter of the head of the connector, and f_y is the nominal tensile yield stress. Because the tensile yield stress of steel of the connectors was not provided in the suppliers' catalogs, yield stress values were therefore taken from the CSA O86-14 (2015) Standard.

Table 1: Connector's dimensions and nominal tensile yield stress.

Type of connector	L (mm)	L_t (mm)	d_i (mm)	d_e (mm)	d_h (mm)	f_y* (MPa)
Roofing nail #11	38.1	-	2.91	2.91	8.66	655
Simpson Strong-Tie HJ	38.1	35.6	3.49	4.70	8.79	550
Rothoblaas TBS 6x80	78.7	46.5	3.88	6.00	13.70	550

* CSA O86-14

The steel deck considered for this particular study is a Canam P-3606 type 22 (Canam 2015). The type 22 deck as a nominal thickness of 0.76 mm that is typically used in commercial and industrial low-rise building structures. The sheet steel normally used for Canam decks profiles correspond to ASTM A653M SS Grade 230 (ASTM A653/A653M-09 2009) with nominal tensile yield stress f_y = 230 MPa and ultimate tensile stress f_u = 310 MPa. In order to get a better estimate of the "true" values of f_y and f_u, four tensile coupon tests were performed in compliance with Standard ASTM E8/E8M-09 (2009). The coupon test results revealed an average yield stress $f_{y,exp}$ = 355 MPa and an ultimate tensile stress $f_{u,exp}$ = 466 MPa.

The wood used for this particular study was provided by a local industrial grade wood provider. The type of wood provided is grade no.1 SPF. The properties of the wood were experimentally characterized using ASTM D2395-14 (2014) and ASTM D4442-16 (2016). The measured properties were similar to the design properties provided in the CSA O86-14. In particular, the specific gravity obtained experimentally was 0,40 compared to 0.42 in CSA O86-14.

2.1 Prediction of the lateral yield strength and slip modulus of single shear connections

Attempts were made to calculate the "unit" lateral yield strength and slip modulus (shear stiffness) of single shear connections. The connections were assumed to be laterally loaded relying on steel connector to wood bearing and/or steel connector to steel sheet bearing for transfer of the lateral load. The applied lateral load is perpendicular to the length of the connector.

2.1.1 Lateral yield strength calculated according to CSA O86-14

Over the past sixty years, there has been a great deal of research about the mechanical behavior of dowel type connectors in wood structures. The theoretical basis for the Canadian CSA O86-14 (2014) standard for bolted, pinned, nailed and screwed connections is the European yield model developed by Johansen

(Johansen 1949). This model proposes equations to calculate the lateral yield strength taking into account a wide variety of failure modes. In CSA O86-14, the method for determining elastic strength is based on the work of Whale et al. (1987). The lateral yield strength calculated according to CSA O86-14 comprises seven failure modes, where six of these modes are applicable to connections with a single shear plane. Those failure modes are presented in Figure 1. The lowest strength obtained from these failure modes corresponds to the unit lateral yield strength of the connection. The equations related to these modes are presented in articles 12.9.4 (for nails) and 12.11.4 (for wood screws) of CSA O86-14. In Figure 1, considering that the top element of a connection is a steel sheet and the bottom element is a wood member: mode (a) is a uniform bearing failure in the steel sheet; mode (b) is a uniform bearing failure in the wood member; mode (d) is a combination of steel sheet bearing failure and one or more plastic hinges in the connector; mode (e) is a combination of bearing failure in the wood member and one or more plastic hinge in the connector; mode (f) represents a rigid body rotation the connector with localized crushing of wood fibers and yielding of the steel sheet at the connection interface; mode (g) is a combination of two plastic hinges in the connector with localized crushing of wood fibers and yielding of the steel sheet at the connection interface.

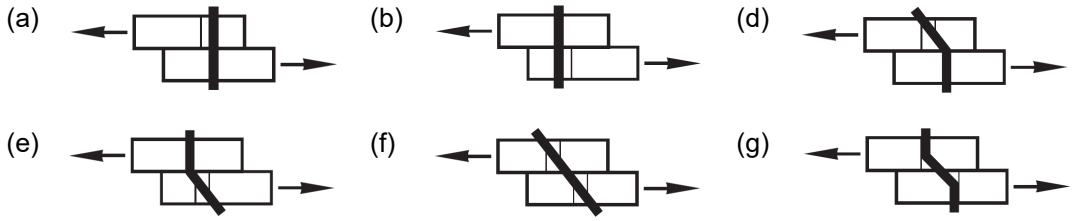

Figure 1: Failure modes applicable to connections with a single shear plane (adapted from CSA O86-14).

The nominal lateral yield strengths, denoted here Q_f as in (Luttrell 2015), were calculated so that they can be compared to the test results. The nominal lateral yield strengths were obtained considering all resistance factors (ϕ) equal to unity, all J factors affecting the resistance of a connection equal to unity, and all modification factors (K) equal to unity, except for load duration factor $K_D = 1.15$ and $K_{sp} = 2.7$ for cold-formed light gauge steel referenced in CSA S136-16 (2016). Because the steel sheet is not made of wood, K_D was only used to modify the embedment strength of the main member (f_2) and the embedment strength of the main member where failure is connector yielding (f_3). The dimensions and mechanical properties of the connectors are presented in Table 1. The mechanical properties of the steel deck material are based on the coupon tests mentioned in Section 2. The wood type considered is SPF no.1 grade with a specific gravity equal to 0.40 corresponding to the value that was measured experimentally. The nominal lateral yield strength of the connections calculated with CSA O86-14 ($Q_{f,O86}$) are presented in Table 2.

Table 2: Nominal lateral yield strength of the connections according to CSA O86-14.

Mode of	Nail #11		SST-HJ		Rotho-TBS	
failure	(N)	% of $Q_{f,O86}$	(N)	% of $Q_{f,O86}$	(N)	% of $Q_{f,O86}$
(a)	2746	323%	3298	294%	3664	265%
(b)	2425	285%	2895	258%	6684	484%
(d)	974	115%	1220	109%	1423	103%
(e)	27340	3215%	32882	2934%	75633	5479%
(f)	1034	122%	1239	111%	2070	150%
(g)	850	100%	1121	100%	1381	100%
$Q_{f,O86}$	**850**	-	**1121**	-	**1381**	-

For each connector, the lateral yield strength value of a particular mode of failure is compared to the strength of the critical mode of failure in terms of percentage. In the cases of the nail and SST-HJ

connectors, the lateral yield strength values corresponding to failure modes (d), (f) and (g) were very close. In the case of the Rotho-TBS connector, modes (d) and (g) yielded almost the same nominal lateral yield strength values. For all connectors, the CSA O86-14 nominal lateral yield strength corresponds to mode of failure (g). As expected, the Nail #11 exhibited the lowest strength, and the Rotho-TBS exhibited the highest strength having the largest gauge and embedment length among the three connectors. The nominal lateral yield strengths calculated according to CSA O86-14 will be compared to experimental results in Section 5.

2.1.2 Lateral yield strength calculated according to AISI S310-13

Standard AISI S310-13 considers the nominal lateral yield strength of a steel sheet to wood connection to be the least of: 1) nominal shear strength of the connection limited by bearing of the screw or nail against either the wood support (mode (b) of Figure 1) or the steel sheet (mode (a)), and modified in accordance with penetration; and 2) nominal shear breaking strength of screw or nail, as applicable, as reported by the manufacturer or determined by independent laboratory testing. The nominal lateral yield strength of the connections calculated with AISI S310-13 ($Q_{f,S310}$) are presented in Table 3.

Table 3: Nominal lateral yield strength ($Q_{f,AISI}$) of the connections according to AISI S310-13.

Mode of	Nail #11		SST-HJ		Rotho-TBS	
failure	(N)	% of $Q_{f,S310}$	(N)	% of $Q_{f,S310}$	(N)	% of $Q_{f,S310}$
(a)	2267	191%	3662	170%	4675	184%
(b)	1188	100%	2155	100%	2544	100%
$Q_{f,S310}$	**1188**	-	**2155**	-	**2544**	-

The nominal lateral yield strength values obtained with AISI S310-13 are much higher than those obtained from CSA O86-14. These values will be compared to experimental results in Section 5.

2.2 Prediction of the slip modulus

Unfortunately, there are no equations in the CSA O86-14 Standard to predict the slip modulus in the elastic range (effective shear stiffness) of the connections. However, AISI S310-13 and Eurocode 5 (2008) propose equations to evaluate slip modulus values for the type of connection that is considered herein. The slip modulus values calculated according to these two references will be presented and compared to experimental values in Section 5.

2.2.1 Slip modulus calculated according to AISI S310-13

The slip modulus $K_{f,S310}$ of wood screws (or nails) fastened through the bottom flat of the steel deck and into wood support is presented in Equation 1. The slip modulus $K_{f,S310}$ is equal to the inverse of the connection's flexibility S_f (Luttrell 2015):

[1] $$K_{f,S310} = (S_f)^{-1} = \frac{1000\sqrt{t}}{1{,}15\alpha} \text{ N/mm,}$$

where the slip modulus is proportional to the square root of the thickness of the steel sheet (t), and $\alpha = 28.8 \times 10^{-3}$ for SI units.

2.2.2 Slip modulus calculated according to Eurocode 5

Eurocode 5 provides equations to evaluate the slip modulus of nailed or screwed connections under service loads (K_{ser}). These equations, provided in table 7.1 of Eurocode 5, are presented in Equation 2 for nails, and Equation 3 for screws. Both equations are functions of the wood's density (ρ_m) in kilograms per cubic meter and the exterior diameter of the connector (d) in millimeters.

[2] $K_{f,EC5} = K_{ser} = 2\rho_m^{1.5}\left(\frac{d^{0.8}}{30}\right)$ N/mm

[3] $K_{f,EC5} = K_{ser} = 2\rho_m^{1.5}\left(\frac{d}{23}\right)$ N/mm

In both cases, as expected, denser wood and larger connector diameters lead to stiffer connections.

3 EXPERIMENTAL INVESTIGATION

The connections built with the three different connectors described in Section 2 were tested to determine their lateral yield strengths and slip modulus. The connectors are presented in Figure 2a). Ten lateral loading tests were performed per connection type for a total of 30 experiments. The experimental test set-up (Figure 2b) was prepared in accordance with the ASTM D1761-12 (2012): "Standard Test Methods for Mechanical Fasteners in Wood". Each specimen consisted of a No. 1 SPF wood member measuring 89 x 113 x 305 mm^3 (3.5 x 4.5 x 12.0 in^3) connected to a 152 mm (6 in.) wide Canam P-3606 22 deck section to include a crest. The steel deck section was 305 mm (12 in) in length. The wood member and the steel deck section were connected together by one connector in single shear. A 1/4" thick steel anchor plate was attached to the wood member by a 1/2" diameter bolt. Another 1/4" steel plate was attached to the steel deck section by means of two 1/4" diameter bolts. Each steel plates were attached to the Instron press that was used. In the case of the nails, the two components were connected using a pneumatic roofing nail gun. In the case of the screws, a power drill equipped with a clutch that was set to apply an 11 N-m torque was used. During a test, a lateral load was applied at a constant displacement rate of 25.4 mm/min (1 in./min). The applied load and slip were recorded using a sampling interval of 10 samples per second. After the tests, the raw data was processed to correct the initial latency and initial connection gaps before the displacement ramp was applied.

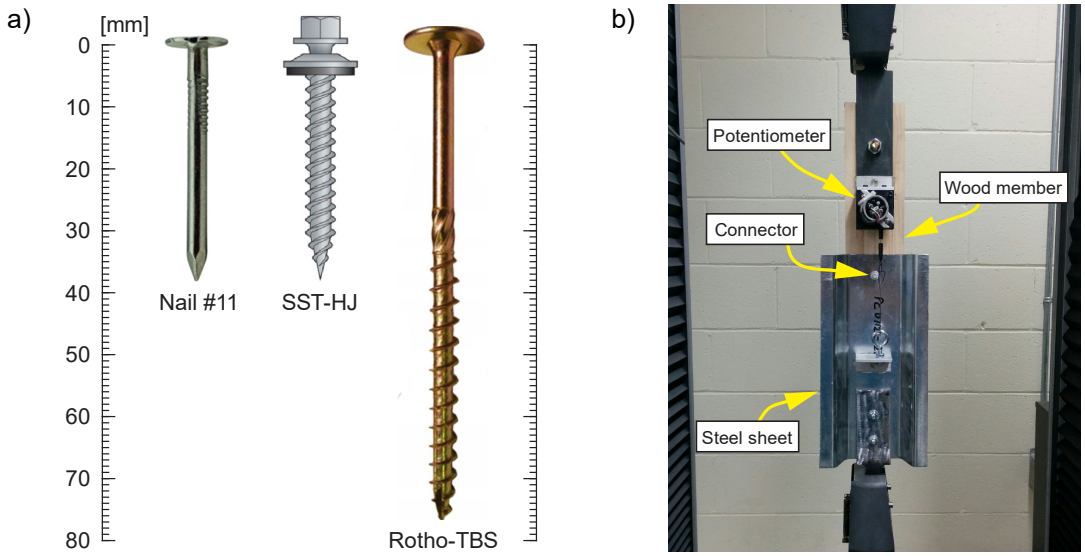

Figure 2: a) Connectors investigated; b) Experimental test set-up and typ. test specimen.

4 EXPERIMENTAL RESULTS

Three typical lateral load vs slip curves are presented in Figure 3, where the ultimate lateral load $Q_{u,exp}$ and lateral yield strength $Q_{f,exp}$ are identified. The lateral yield strength was identified using a slightly modified version of the 5% of diameter method (ASTM D5652 2015) proposed in National Design Specification for Wood Construction (AWC NDS-15 2015). In this method, the yield point is defined as the intersection of a straight line which is parallel to the initial stiffness and the load-slip curve. In the case of the nails, the secant

slope between 10% and 40% of the ultimate load was used. In the case of the screws, the secant slope between 5% and 15% of the ultimate load was used. The slight modification to the 5% of diameter method for the screws was necessary because the behavior of the connection at 40% of the ultimate load was well beyond the linear elastic range. In the three cases, but especially in cases of the screws, lateral yield strength values are underestimated with respect to reality. For hybrid connections, such as those studied herein, the precision of the 5% of diameter method was deemed “questionable” by Muñoz et al. (2008).

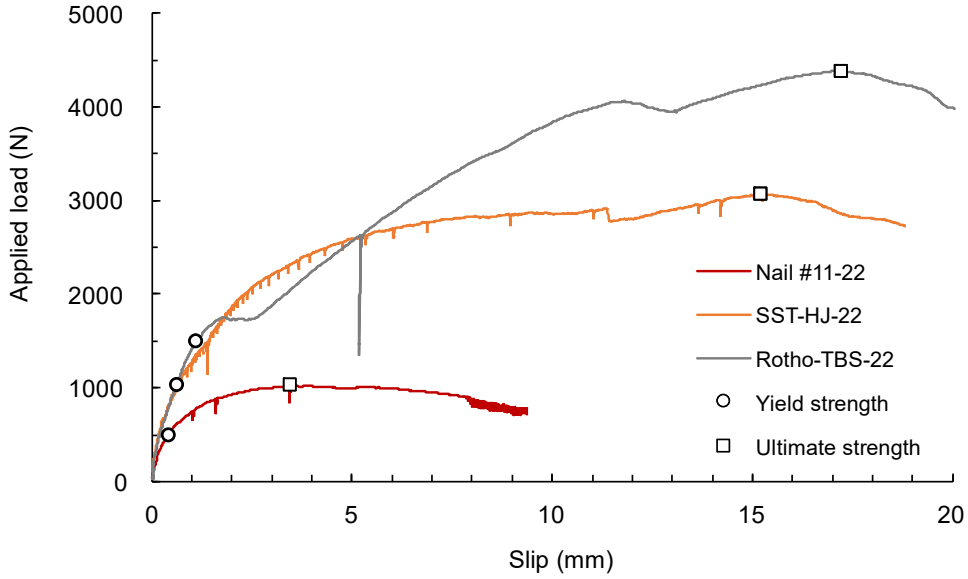

Figure 3: Typical experimental applied force vs slip curves involving the three connectors.

Each curve presented in Figure 3 exhibit a linear elastic behavior up to the attainment of the lateral yield strength of the connection. Thereafter, the load-slip behavior softens and the load gradually increase until the ultimate load is reached. In the case of the Nail #11 connection, the failure mode that was observed is the same as the prediction made in Section 2, i.e., mode (g). This is confirmed by the residual deformation in the nail presented in Figure 4 where two inflection points corresponding to plastic hinges are clearly visible. In the case of the connections using screws, Rotho-TBS failed according to mode (g) and SST-HJ failed according to mode (f), despite the fact that mode (g) was expected to take place in both cases. This can be explained by the fact that the relative differences of the lateral yield strength between mode (f) and expected mode (g) for the SST-HJ screw is only 11 percent (see Table 2). The permanent deformation visible in the cross-cut of the wood pieces taken from the SST-HJ and Rotho-TBS lateral strength tests, presented in Figure 4, confirms that the mode of failures were mode (f), and (g), respectively.

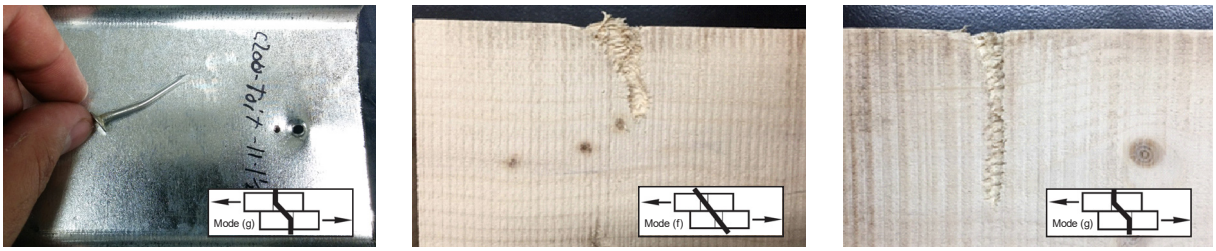

a) b) c)

Figure 4: a) Residual deformations in a nail; Residual deformations in wood: b) SST-HJ, c) Rotho-TBS.

The experimental test results are synthesized in Table 4, where the experimental yield strength $Q_{f,exp}$, ultimate strength $Q_{u,exp}$, and slip modulus K_{exp} are presented along with the ductility factor μ and overstrength ratio $R_o = Q_{u,exp}/Q_{f,exp}$. The ductility level is the ratio between the slip value measured at $Q_{u,exp}$ and the slip values measured à $Q_{f,exp}$. Although this paper aims at evaluating the lateral strengths of the

connections and diaphragms in the linear regime, it is of interest to note that the connections exhibited important ductility levels and reserve capacities which are of great value in the context of a seismic design. For $Q_{u,exp}$ and $Q_{f,exp}$, all coefficients of variation (CV) are inferior to 20%. In the case of K_{exp}, CV values lie between 22.7% and 42.9%.

Table 4: Average experimental test results and coefficients of variation.

	Nail #11		SST-HJ		Rotho-TBS	
	Average	CV	Average	CV	Average	CV
$Q_{f,exp}$ (N)	725	16.8%	1025	10.2%	1125	19.2%
K_{exp} (N/mm)	1131	42.9%	2335	26.8%	1897	22.7%
$Q_{u,exp}$ (N)	1182	17.6%	2985	15.5%	3504	28.0%
μ (mm/mm)	6.8	47.9%	22.0	31.4%	18.2	40.4%
R_o (N/N)	1.65	15.4%	2.97	23.0%	3.12	20.8%

5 COMPARISON BETWEEN PREDICTION EQUATIONS AND TEST RESULTS

The average experimental lateral yield strengths $Q_{f,exp}$ and average experimental slip moduli $K_{f,exp}$ are compared to code predictions in Table 5 and Table 6. From Table 5, it is clear that CSA-O86-14 yields to more precise nominal lateral yield strength predictions than AISI S310-13. The CSA-O86-14 overestimates the lateral yield strengths by 9 to 23 percent. AISI S310-13 predictions overestimate the lateral yield strengths by 64 to 226 percent. In the case of the slip modulus, Eurocode 5 overestimates average experimental values by 11 to 40 percent. AISI S310-13 predictions overestimate slip moduli by 1127 to 2327 percent. The very important discrepancies between the AISI S310-13 predictions and the test results are due to the fact that Equation 2 is based on lateral yield strength tests on the steel structures.

Table 5: Comparison between nominal lateral yield strength predictions and experimental test results.

	Nail #11 (N)			SST-HJ (N)			Rotho-TBS (N)		
	$Q_{f,exp}$	Q_f	$Q_f/Q_{f,exp}$	$Q_{f,exp}$	Q_f	$Q_f/Q_{f,exp}$	$Q_{f,exp}$	Q_f	$Q_f/Q_{f,exp}$
CSA-S16-14	725	850	1.17	1025	1121	1.09	1125	1381	1.23
AISI S310-13	725	1188	1.64	1025	2155	2.10	1125	2544	2.26

Table 6: Comparison between slip modulus predictions and experimental test results.

	Nail #11 (N/mm)			SST-HJ (N/mm)			Rotho-TBS (N/mm)		
	$K_{f,exp}$	K_f	$K_f/K_{f,exp}$	$K_{f,exp}$	K_f	$K_f/K_{f,exp}$	$K_{f,exp}$	K_f	$K_f/K_{f,exp}$
Eurocode 5	1131	1253	1.11	2335	3270	1.40	1897	4174	2.20
AISI S310-13	1131	26322	23.27	2335	26322	11.27	1897	26322	13.88

It is clear from Tables 5 that the AISI S310-13 prediction are not conservative in evaluating the strength of the connections. In the case of the CSA O86-14 standard, the strength predictions are satisfactory, but slightly unconservative. Nevertheless, it should be reminded that the lateral yield strength identified experimentally with the modified 5% diameter method are conservative with respect to the “true strength” of the connection (see Section 4).

6 STRENGTH AND STIFFNESS OF A STEEL DECK TO WOOD FRAME DIAPHRAGM

Steel diaphragms are planar structural systems found mainly in roofs, floors and walls of buildings. The main components of a diaphragm consist of individual steel deck panels that are attached to the main and

secondary structural elements using appropriate connectors. Types of connectors include nails, screws, welds (in steel structures) and other mechanical devices with predictable capacities. The in-plane strength and stiffness of a steel deck diaphragm depend on the geometrical and mechanical properties of the deck panels, the layout of the supporting members and connections, and the mechanical properties of those connections. The diaphragm considered herein are composed of 38 mm deep and 0.76 mm thick Canam P3606 steel deck sheets (Canam 2015). Each sheet is 914 mm wide, with flutes spaced at 152 mm. Each sheet is 6000 mm long and lies over 5 equal spans between the joists that are positioned at 1200 mm c/c of each other. Two fastening patterns are considered: 1) 914/4 pattern (36/4 in imperial units) with single side-lap screws disposed at every 600 mm along the length of the side-lap (light pattern); and 2) 914/11 pattern (36/11 in imperial units) with single side-lap screws disposed at every 150 mm along the length of the side-lap (dense pattern). The number of fasteners is the same at the exterior and interior supports and the spacing of the intermediate side-lap connectors is the same as it is at the outside edge of the building. The shape of the steel deck and the connection patterns are presented in Figure 5.

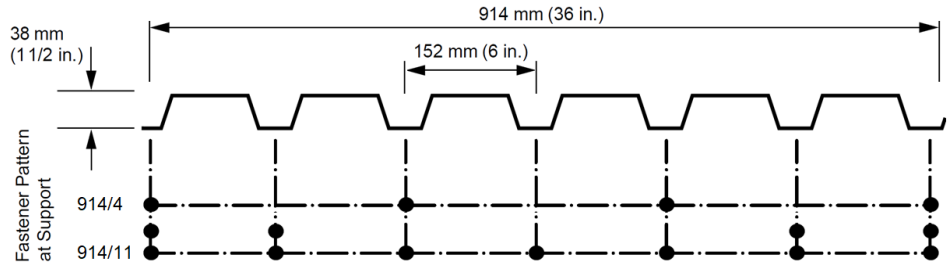

Figure 5: Steel deck connector patterns per panel at supports (adapted from Canam (2015))

The connectors considered to connect steel sheets to wood supports are those presented in Section 2. The connectors used to connect steel sheets to steel sheets (side-laps) are #10 Hilti HWH self-tapping screws (Hilti 2018). The three steel sheets to wood connectors and the two fastening patterns considered lead to six steel decks to wood frame diaphragm designs. In addition to the steel deck to wood frame diaphragms, two other diaphragms were designed considering steel members instead of wood members for comparison purposes. For these designs, Hilti X-HSN 24 frame fasteners (Hilti 2018) and the same #10 Hilti HWH self-tapping screws used in the steel decks to wood frame cases were considered. The nominal strength and stiffness of each connector considered in the designs are presented in Table 7.

Table 7: Nominal lateral yield strength and slip modulus considered in design.

Connector	Function*	Q_f (N)	K_f (N/mm)	S_f (mm/kN)
Nail #11	SS	725	1031	0.9699
SST-HJ	SS	1025	2235	0.4474
Rotho-TBS	SS	1125	1897	0.5271
Hilti X-HSN 24	SS	6640	23989	0.0417
Hilti #10 HWH**	SL	2823	10007	0.0999

*: Steel deck to structure connector (SS); Side-lap connector (SL); **: Q_s, K_s and S_s.

The nominal shear strength and stiffness of the steel deck to wood connections correspond to the experimental values presented in Section 4. The nominal shear strength and stiffness of the Hilti connectors are based on the manufacturer's technical data (Hilti 2018). The mechanical properties of the steel deck sheets considered are the same as those experimentally measured in the steel deck to wood connections, i.e. f_y = 355 MPa (51.5 ksi) and an ultimate tensile stress f_u = 466 MPa (67.6 ksi). All diaphragms were designed in accordance with the limit state design approach using the SDI method (Luttrell 2015) that conforms to AISI-S310-13 (2013) and AISI-S100-16 (2016). The resistance factors used are based on AISI S310-13, where ϕ_d = 0.5 for the fasteners into wood support and Hilti fasteners (Luttrell 2015) under all load cases, and ϕ_d = 0.75 for panel buckling.

The design strengths per unit length S_n of the diaphragms are presented in Table 8 where it is clear that the steel to steel designs are 3 to 5 times stronger than the steel to wood designs for the same fastening pattern. Nevertheless, a similar strength can be achieved with a steel to wood design if a denser fastening pattern is used compared to its steel to steel counterpart. E.g., a 914/11-150 mm steel to wood diaphragm using SST-HJ screws is slightly stronger compared to its 914/4-600 mm steel to steel counterpart. As expected, strength-wise, the steel to wood diaphragm designs using the screws performed similarly and performed better than the steel to wood diaphragms using Nail #11. Though the diaphragms using Nails #11 are less efficient than all other solutions, their unit cost and installation cost might make them an interesting solution from an economical perspective. The shear stiffnesses *G*' of the steel to wood and steel to steel diaphragms are presented in Table 9 where it can be observed that all steel to wood solutions have similar shear stiffnesses for a given fastening pattern. For equivalent fastening patterns, steel to steel solutions yield to *G*' values between 12 and 27 percent in excess of their steel to wood counterparts. The discrepancies between the *G*' resulting form the use of different connectors for a given fastening pattern are much lower than in the case of S_n. This is due to the fact that the shear flexibility of the diaphragms is governed by shear deformations in the steel decks.

Table 8: Design strengths of the steel to wood and steel to steel diaphragms.

	Pattern 914/4 - 600 mm			Pattern 914/11 - 150 mm		
Connector	S_n (N/mm)	$S_n/S_{n,Rotho}$	$S_n/S_{n,Hilti}$	S_n (N/mm)	$S_n/S_{n,Rotho}$	$S_n/S_{n,Hilti}$
Nail #11	0.78	63.9%	18.0%	3.44	65.8%	21.6%
SST-HJ	1.11	91.0%	25.6%	4.86	92.9%	30.5%
Rotho-TBS	1.22	100.0%	28.2%	5.23	100.0%	32.8%
Hilti X-HSN 24	4.33	354.9%	100.0%	15.95	305.0%	100.0%

Table 9: Shear stiffnesses of the steel to wood and steel to steel diaphragms.

	Pattern 914/4 - 600 mm			Pattern 914/11 - 150 mm		
Connector	G' (kN/mm)	G'/G'_{Rotho}	G'/G'_{Hilti}	G' (kN/mm)	G'/G'_{Rotho}	G'/G'_{Hilti}
Nail #11	2.99	98.0%	77.3%	15.64	99.3%	88.4%
SST-HJ	3.08	101.0%	79.6%	15.80	100.3%	89.3%
Rotho-TBS	3.05	100.0%	78.8%	15.75	100.0%	89.0%
Hilti X-HSN 24	3.87	126.9%	100.0%	17.70	112.4%	100.0%

7 CONCLUSIONS

Three different dowel type connectors were investigated in order to connect steel decks to structural wood members. The lateral yield strengths and slip modulus of the connections were calculated using equations available in current design codes and standards. These predictions were compared to lateral load test results where it was found that CSA O86-14 could predict the nominal yield strength of the connections with good accuracy, whilst the prediction made with AISI S310-13 yielded to largely overestimated predictions. In this particular study, Eurocode 5 equation for predicting the slip modulus of nailed connections was found to be accurate, but Eurocode 5 equation for screwed connections led to slip modulus values that ranged between 140 to 200 percent of the measured values. The equations proposed by AISI S310-13 to predict the slip modulus lead to predictions that are more than ten times higher than the experimental values. Out of the three connectors investigated, the screws exhibited better strength and stiffness properties compared to the nails. Every connection tested exhibited a ductile behaviour and had reserve capacity past their yield strength. These features are great assets in the context of a seismic design.

Based on the connections test results, the design shear strength S_n and shear stiffness *G'* of steel decks to wood frame diaphragms were calculated. Light and dense fastening patterns were considered. For this particular case study, the steel to steel designs were 3 to 5 times stronger than the steel to wood designs

for a given fastening pattern. The shear stiffnesses *G'* of the steel to wood and steel to steel diaphragms had similar shear stiffnesses for a given fastening pattern. This is due to the fact that the shear flexibility of the diaphragms is governed by shear deformations in the steel decks. As expected, strength-wise, the steel to wood diaphragm designs using the screws performed similarly. The steel to wood diaphragm using screwed connections performed better than those with common roofing nails. Though the diaphragms using nails were less structurally efficient than all other solutions, their unit and installation costs might make them an interesting solution from an economical perspective. The steel deck to wood frame diaphragm presented in this paper showed great potential. More research on the strength and behavior of the connections and large-scale diaphragm tests should be performed in order to use steel deck to wood frame diaphragm in a practical context.

8 ACKNOWLEDGEMENTS

Funding for this research was provided by Structure Fusion (Canam), Mitacs, Natural Sciences and Engineering Research Council of Canada (NSERC), Fonds de Recherche Nature et les Technologies du Québec (FRQNT), and Canada Foundation for Innovation. The authors wish to express their appreciation to Claude Aubé and the technical staff members of Université de Sherbrooke's structural laboratory.

9 REFERENCES

AISI S100-16. 2016. North American Standard for Design of Cold-Formed Steel Structural Members, American Iron and Steel Institute (AISI), Washington, DC.

AISI S310-13. 2013. North American Standard for the Design of Profiled Steel Diaphragm Panels, American Iron and Steel Institute (AISI), Washington, DC.

ASTM A653/A653M-09. 2009. Standard Specification for Steel Sheet, Zinc-Coated (Galvanized) or Zinc-Iron Alloy-Coated (Galvannealed) by the Hot-Dip Process. ASTM Int., West Conshohocken, PA, USA.

ASTM D1761-12. 2012. Standard Test Methods for Mechanical Fasteners in Wood. ASTM International, West Conshohocken, PA, USA.

ASTM D2395-14. 2014. Standard Test Methods for Density and Specific Gravity (Relative Density) of Wood and Wood-Based Materials. ASTM International, West Conshohocken, PA, USA.

ASTM D4442-16. 2016. Standard Test Methods for Direct Moisture Content Measurement of Wood and Wood-Based Materials. ASTM International, West Conshohocken, PA, USA.

ASTM D5652-15. 2015. Standard Test Methods for Single-Bolt Connections in Wood. ASTM International, West Conshohocken, PA, USA.

ASTM E8/E8M-09. 2009. Standard Test Methods for Tension Testing of Metallic Materials. ASTM International, West Conshohocken, PA, USA.

AWC NDS-15. 2015. National Design Specification for Wood Constr., American Wood Council, VA, USA.

Canam. 2015. Steel Deck Diaphragm: Technical Catalogue. Groupe Canam, St-Georges, Qc, Canada.

CSA O86-14. 2015. Eng. design in wood. Canadian Standard Association (CSA) Group, Toronto, ON.

CSA S136-16. 2016. North American specification for the design of cold-formed steel structural members, CSA Group, Toronto, ON.

Eurocode 5. 2018 Design of timber structures - Part 1-1. European Comm. for Stand., Brussels, Belgium.

Hilti. 2018. North American Product Tech. Guide, Vol. 1. Ed.18. Hilti inc., Tulsa, OK, USA.

Johansen, K.W. 1949. Theory of timber connections. IABSE publications 9: 249-262.

Luttrell, L.D. 2015. SDI Design Manual, 4nd ed., Steel Deck Institute (SDI), Fox River Grove, IL.

Muñoz, W., Mohammad, M. and Salenikovich, A. 2008. "Determination of yield point and ductility of timber assemblies: in search for a harmonised approach." 10th World Conf. on Timber Engineering, Japan.

Rothoblaas. 2018. Screws and connectors for wood: Technical Catalogue. Cortaccia, TN, Italia.

Simpson Strong-Tie. 2018. Fastening Systems catalog: Technical Catalogue. Brampton, ON, Canada.

Whale, L.R.J., Smith I., and Larsen. H.J. 1987. Design of nailed and bolted joints proposals for the revision of existing formulae in draft EC5 and the CIB code. Proc. of the CIB-W18 Meeting. Dublin, Ireland.